Acoustic estimation of size distribution and abundance of zooplankton

Åge Kristensen

Continental Shelf and Petroleum Technology, Research Institute Ltd., Håkon Magnussonsgt 1B, P. O. Box 1883, N-7001 Trondheim, Norway

John Dalen

Institute of Marine Research, Directorate of Fisheries, P. O. Box 1870, N-5011 Bergen, Norway

A series of investigations were undertaken to observe and describe the sound backscattering process from larger zooplankton (*euphausiids*). The target strength versus frequency, size, and aspect angle of the organism was measured. The target strength is highly dependent on the density and sound speed contrasts between the target and the medium, and both these parameters were measured. From the target strength observations it was concluded that the fluid sphere model was insufficient as a scattering model for krill. Observations of the tilt angle distribution of krill at natural field conditions showed that they were distributed over a large region of tilt angles. The deficiencies of the fluid sphere models required the development of a new scattering model based on experimental data. This model predicts a decreasing target strength versus frequency in the geometric scattering region. The backscattering spectra of *euphausiids* were better described by our empirical model than by the fluid sphere models. Applying the empirical model to estimate size distribution and biomass of krill, we found strong correlation between the acoustically estimated distributions and those from net catches.

PACS numbers: 43.30.Bp, 43.30.Gv, 43.80.Jz

INTRODUCTION

Estimation of zooplankton abundance, size distribution, and species composition is important for the understanding of the biological processes and the resources of the ocean. At present, such information is dependent mainly on zooplankton sampling using various types of plankton nets. Net sampling involves a high proportion of inaccuracy due to patchiness,[1,2] net avoidance, and clogging.[3]

In acoustic estimation of zooplankton populations essentially two basic approaches have been tried. In the first approach, the data from biological samples, from net and trawl catches, along with acoustic measurements at a single frequency, are used to establish a regression equation.[4] This regression equation is then used to convert measured volume backscattering strength into zooplankton biomass. Extraction of information of size distribution, from the acoustical data, is beyond the scope of this method.

In the second approach, a multifrequency scattering model for the investigated zooplankton species has to be known. The model can be empirical or theoretical.[5–8] The target strength predicted by these models is generally dependent on the frequency, size, and the density and sound speed contrasts between the organism and the medium. The physical shape of the organisms may also be introduced as a parameter. If the target strength of the zooplankton under investigation is known as a function of both frequency and size and also meets certain criteria for nonsingularity, the size distribution and biomass can be estimated by using a multifrequency sonar system.

This article will deal with the second approach. The existing models will be reviewed and an empirical scattering model will be presented.

I. SCATTERING MODELS

A. Volume backscattering

Backscattering of the acoustic intensity from a single target can be described by the backscattering cross section[9] σ_{bs} or the target strength TS. When dealing with backscattering from a volume with many scatterers, the volume backscattering coefficient s_v and the volume backscattering strength S_v are commonly used.

In general, the backscattering cross section of a target is a function of the size, the physical parameters, the orientation of the scatterer, and the frequency of the acoustic system. For *euphausiids*, it has been experimentally demonstrated that the backscattering cross section is a function of the orientation, only in the head–tail aspect and not in the dorsal–lateral aspect.[7,10]

In this work we assume that all the size groups have the same angular distribution function and calculate a mean backscattering cross section,

$$\bar{\sigma}_{bs,m}(f) = \sigma_{0,m}(f) \sum_{k=1}^{K} n_k d_k, \qquad (1)$$

where

$\sigma_{0,m}(f)$ = backscattering cross section at a reference orientation O and frequency f of size group m,

n_k = relative number of organisms per m³ of orientation group k, defined such that $\Sigma_{k=1}^{K} n_k = 1$,

d_k = orientation function of the organisms of orientation group k,

K = the number of orientation groups.

In real situations, the received backscattered intensity is composed of contributions from many individual organisms, which simultaneously contribute to the total echo. Based on the assumption that the objects are randomly distributed in space, the volume backscattering coefficient s_v will simply be the sum of the backscattering cross section σ_{bs} of each organism.

If we take into account the relative length-frequency distribution of the scatterers, the volume backscattering coefficient may be written

$$s_v = N \sum_{m=1}^{M} \bar{\sigma}_{bs,m} \ (f)l_m, \qquad (2)$$

where

N = total number of scatterers per m^3,

M = number of size groups,

l_m = relative number of scatterers of the mth size group, defined such that $\Sigma_{m=1}^{M} l_m = 1$.

B. Multifrequency scattering models

When working with a multifrequency acoustic system, it may be possible to obtain information of the zooplankton size distribution if a model of the target strength, as a function of frequency and size, exists.

A relevant theoretical model for calculating the target strength of zooplankton is that of a fluid sphere.[5] This model has been applied, with some success, to predict the volume backscattering strength of copepods[11] and to estimate size distribution of krill.[8]

1. The fluid sphere model

By a fluid sphere, we mean a spherical particle which can be penetrated by an incident acoustic wave. An implication of the fluid assumption is that only compressional waves exist in the interior of the particle.

In Fig. 1 the Anderson,[5] Johnson,[6] and Rayleigh[12] models are compared for a fluid sphere of the same size and physical properties. In the low-frequency region, $ka < 1$, the Anderson solution is exactly the same as that derived by Rayleigh. In this region the backscattering cross section is highly dependent on the frequency (to the fourth power) and the size (to the sixth power) of the scatterer. In the high-frequency region, $ka > 1$, the geometrical scattering region, the backscattering cross section is a complex function of the frequency, containing several maxima and minima. The minima and maxima in the Anderson model are caused by constructive and destructive interference of the different scattering modes. These phenomena will only occur for particles of high symmetry such as spheres, cylinders, spheroids, and so forth. Relatively complicated computations must be performed to predict target strength from the Anderson model. The geometry of the zooplankton species we are interested in, copepods and euphausiids, is far from a sphere. Therefore, an approximate model for the scattering from zooplankton has been proposed by Johnson. He formulated a function including the first-order approximation at
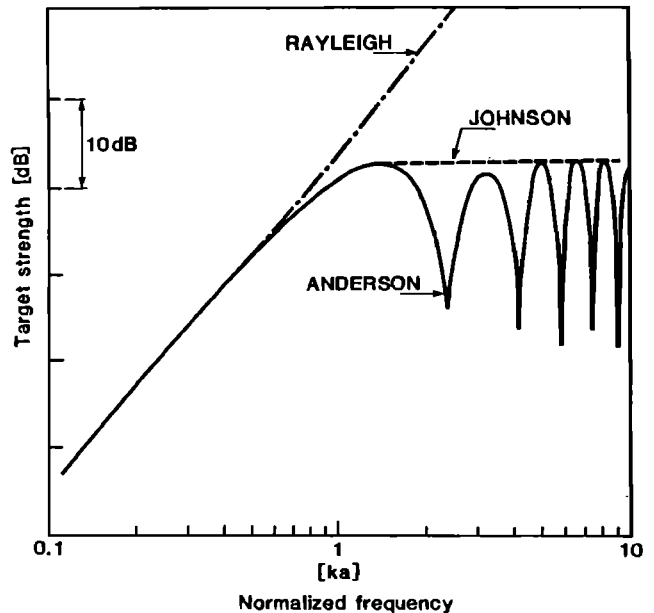

FIG. 1. Comparison of the target strength predicted by the three models (Rayleigh, Anderson, and Johnson) for a 10-mm-radius sphere. The wave-number k is a size parameter. The density and sound speed contrasts are $g = 1.05$ and $h = 1.05$.

low frequencies and having an asymptotic value at high frequencies that is consistent with the maxima of the Anderson model.

2. Other scattering models

In both the Anderson and Johnson models the backscattering cross section is a function of the size of the sphere, its physical properties, and the frequency. In both models, however, the backscattering cross section is independent of the angular orientation of the object, in relation to the incident sound field. This means that it is insufficient to apply such models on directive scatterers. Experimental results reported[7,10] that krill are strongly directive scatterers. This suggests that better scattering models would be provided by ellipsoids, prolate spheroids, and perhaps cylinders. An analytic solution of scattering from a prolate spheroid exists,[13] but this solution is neither favorable for real-time data processing nor for numerical calculations.

Numerical models such as the T-matrix approach[14] or the space-time integral equation method (STIE)[15] are applicable for scattering calculations from targets of arbitrary three-dimensional shape. Elastic properties of the target can be included in these models. Thus scattering computations are not restricted only to fluid particles. However, as the elastic properties of zooplankton are not known, the value of using one of these models is limited.

II. EXPERIMENTAL METHODS, RESULTS, AND DISCUSSION

All the zooplankton specimens which have been used in this work were captured in two neighboring fjords, Balsfjorden and Ullsfjorden, near Tromsø, in northern Norway.

A. Measurements of the target strength of *euphausiids*

1. The method

The experimental method is described in Kristensen and Dalen.[10] When comparing our experimentally measured target strengths with those predicted from the fluid sphere model, we used a sphere with the same volume as that of the krill. We applied a volume–length relation[16] to estimate the equivalent radius a of the sphere,

$$a = 0.136 \times TL^{1.05}, \qquad (3)$$

where

TL = the length of a krill from the anterior margin of the eye to the tip of the telson, in meters.

The frequency range for the target strength measurements was chosen to be from 30 kHz to 1 MHz based on the practical size of the transducers, the nearfield extension, and the location of the transition regions from Rayleigh to geometric scattering for krill lengths between 10–50 mm, as predicted from the fluid sphere model. The target strength was calculated by estimating the mean square value of the stationary part of the backscattered pressure pulse, averaged over 25 pulses at each frequency. The standard deviation at all frequencies was calculated for each measuring series, i.e., for each specimen the s.d. was less than 1.5 dB, highest for the smallest organisms. We assume that this pulse-to-pulse variation occurred because of minor changes in the orientation of the organisms relative to the acoustic beam.
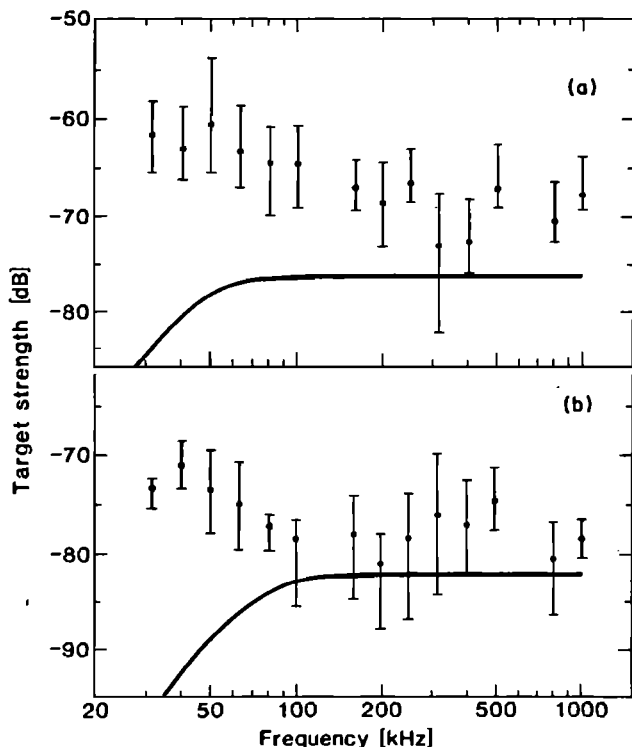

FIG. 2. The measured target strength versus frequency for krill in dorsal aspects. The vertical bars indicate the total range of measured values at each frequency and the dots show the mean values for all specimen. Data for two different bodylengths are shown along with the predictions from the Johnson scattering model (solid lines). (a) 40-mm mean bodylength. (b) 27-mm mean bodylength.
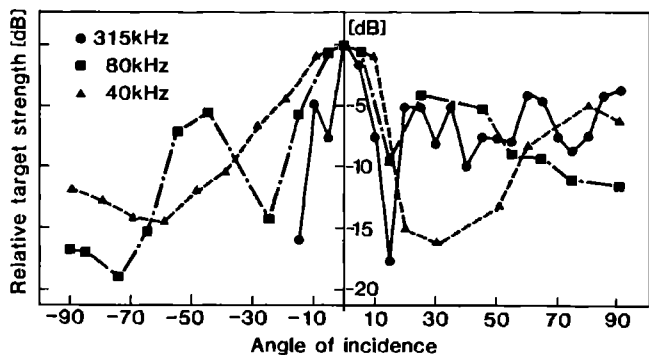
2. The results and discussion

The target strength versus frequency was measured for two size classes containing 16 and 22 specimens. Measurements were done in the lateral and dorsal aspects of the krill and on both fresh and nitrogen-frozen specimens. No significant difference in the target strength was found either for the lateral and dorsal aspects or between fresh and preserved krill. The combined results of the measurements are given in Fig. 2. The smallest size class is *Thysanoessa sp.* with bodylengths of 26–28 mm. The largest size class is *Meganyctiphanes norvegica* with bodylengths of 39–41 mm.

The two size classes of the two different species of krill are physiologically and geometrically quite similar. The biochemical composition and hence, the physical parameters, i.e., the density and sound speed contrasts, are different, as will be discussed later.

In Fig. 2 we have compared the measured target strength versus frequency with that predicted by the Johnson model. The measured target strength in the high-frequency region is about 6 dB higher than the predicted values for both size classes, while, in the low-frequency region, the measured values indicate a resonance at a lower frequency than the predicted transition region. From the Johnson model we find that the predicted target strength difference is 6.6 dB for the two size classes. The measured difference of the mean target strength is about 7–11 dB at all frequencies. Under the assumption of similar scattering properties, the expected difference in target strength should be given by the geometrical cross sections only. This assumption yields a difference of about 3 dB. The remainder is due to differences in the physical parameters between the two krill groups, which will be demonstrated later.

In the acoustic determination of size distribution, the transition region from Rayleigh to geometric scattering should be located. However, our results do not indicate any transition region for the large size class, while for the small size class this region seems to be located at approximately 40 kHz. The model predicts the transition frequencies to be at 48 and 79 kHz for the large and small specimens, respectively. The observed transition region, compared to the prediction from the model, yields a downward shift in frequency of about 50% for the small size class. This may have several causes. An obvious one is that the model treats the interior of the object as a fluid, i.e., ignoring the elastic properties of the object. The effect of the carapace is also omitted. Another cause is the great discrepancy between the spherical geometry of the model and that of the investigated *euphausiids* which are elongated in shape.

Based on the same relative shift in frequency, the expected transition region for the large size class would be approximately 24 kHz. This is below the frequency region of our experiment, so further conclusion about the validity of this expected value cannot be drawn. The target strength versus frequency, observed for the two classes, shows approximately the same frequency dependency. There is a trend of decreasing values with increasing frequency in the region just above the resonance region. At higher frequencies, the target strength tends to vary around a constant value. The general features of the target strength versus frequency are quite

FIG. 3. Normalized target strength of a 43-mm bodylength krill versus angle of incidence at three frequencies. The angle — 90° represents tail aspect and + 90° represents head aspect.

similar to those reported earlier for *euphausiids*.[7]

Orientation-dependent target strength of *euphausiids* is expected. This is caused by the elongated shape of these organisms and the typical wavelengths. Figure 3 shows the normalized target strength of a krill of 43-mm total bodylength versus angle of incidence at three frequencies.

The target strength versus aspect angle shows a relatively well-defined main lobe at the lateral aspect for all three frequencies. As expected, the lobe width increases with decreasing frequency. At other aspects the target strength is rather variable.

B. Measurements of the specific density of *euphausiids*

1. The method

The specific density of zooplankton was measured using a calibrated gradient column method.[17] The accuracy of this method is discussed in Kristensen[18] and is assumed to be within 0.1%.

The individual krill was anesthetized in a 50‰ NaCl solution, identified, and measured before it was put into the column.

2. The results and discussion

Density measurements have been performed on the three most abundant krill species in Norwegian fjords. These are *Thysnoessa raschii*, *Thysanoessa inermis*, and *Meganyctiphanes norvegica*. The two *Thysanoessa* species are physically and biochemically similar. Therefore, the results for these two species were combined. Figure 4 indicates a decrease in specific density as a function of total bodylength. The linear regression equations for the density contrast are given in Eq. (4). We have used a reference density of seawater $\rho_0 = 1.026$ g/cm^3.

$$\text{Thysanoessa sp.} \quad g = 1.058 + 1.30 \times 10^{-3} \times TL. \quad (4a)$$

$$M.\ norvegica \quad g = 1.063 + 7.29 \times 10^{-4} \times TL. \quad (4b)$$

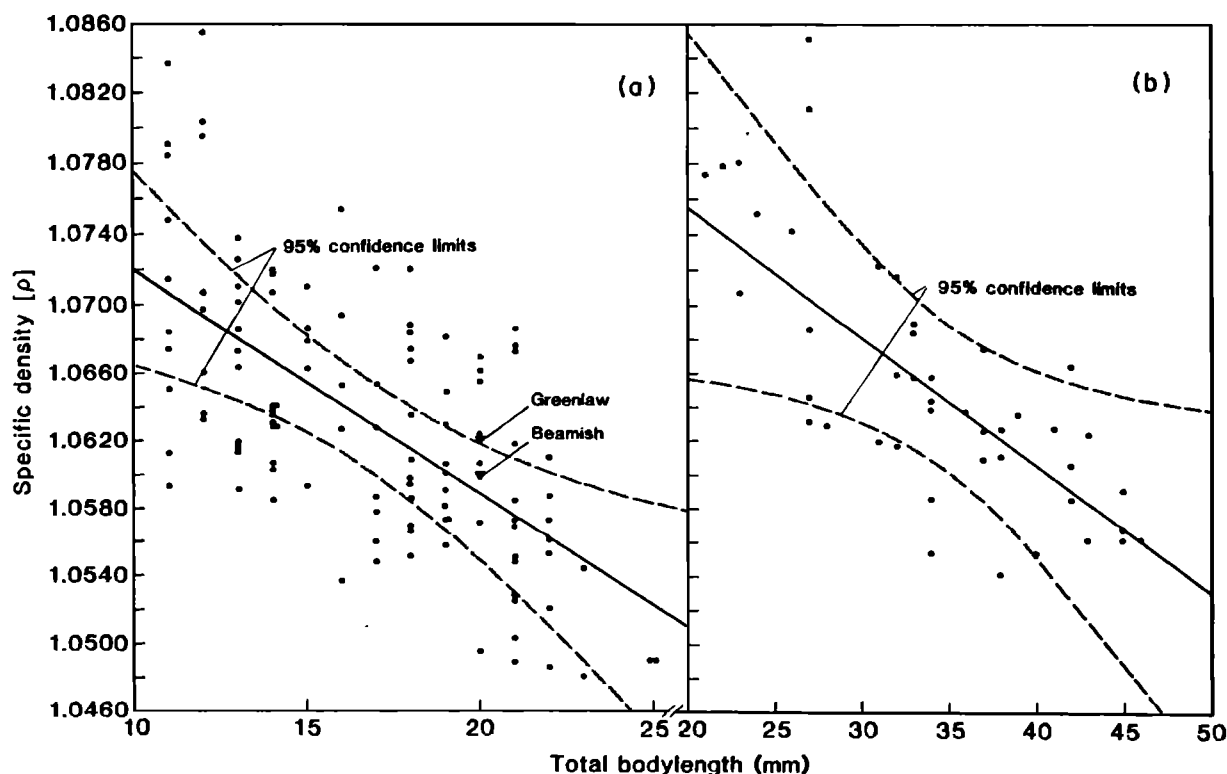A decreasing density versus size is expected, due to the

FIG. 4. Specific density versus length for two different krill species. Regression lines and 95% confidence bands are also shown. (a) *Thysanoessa sp.* (b) *Meganyctiphanes norvegica*.

size-dependent biological composition,[19,20] i.e., lipids and ash content of the krill.

Greenlaw[7] reported a density of 1.063 g/cm³ for live euphausiids (*Euphausia pacifica*)and 1.043 g/cm³ for formalin preserved specimens. These values are the mean densities for krill of 19–23-mm total bodylength. Beamish[21] reported a density of 1.06 g/cm³ for live *E. superba*. Although the measurements of Greenlaw and Beamish were performed on other species and at other latitudes than our measurements, we can see that their results fall close to the upper 95% confidence limit of our measurements on the *Thysanoessa* species, as can be seen in Fig. 4. Compared to *M. norvegica*, their results are considerably lower.
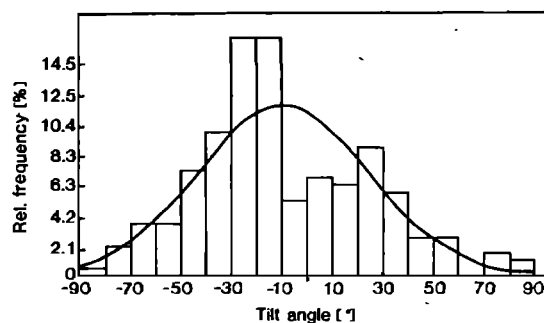

FIG. 5. Relative frequency distribution of tilt angles of krill observed by photocamera. Negative angles are head down. The total number of organisms analyzed is 192. The solid line is the best fit Gaussian distribution.

C. Measurements of the sound speed of *euphausiids*

1. The method

The sound speed of zooplankton was measured as described by Greenlaw.[7]

It was impossible to identify and measure the length of the number of specimens required by this method and simultaneously keep them alive. We found it of little value to measure the sound speed of dead organisms. Therefore, we had to measure the sound speed contrast on mixtures of the *Thysanoessa* species, consisting of approximately 50% of each. The measurements on *M. norvegica* were done on unmixed samples. The sound speed has not been measured, as a function of length, for any of the species.

2. The results and discussion

Several measuring series were performed on both species (see Table I). In the regression analysis of each measuring series the correlation coefficient was higher than 0.98. Sound speed contrast measurements have been reported by Greenlaw[7] on *Euphausia pacifica*. His results on *E. pacifica* of 1.033 agree well with our results on *M. norwegica*.

D. Observation of the spatial orientation of *euphausiids*

1. The method

The demonstrated orientation dependency of the target strength requires some knowledge of the orientation distribution of the organisms in the ocean. Underwater photocamera systems have been used to study this orientation distribution.[21,23] We used a photocamera system mounted on the transducer frame. The camera was triggered from the surface, upon favorable conditions, by the density of plankton in front of the system. Only krill located in the focal

plane of the camera, clearly oriented broadside to the camera, were analyzed with respect to their tilt angles. The tilt angle was defined as the angle between the horizontal and a line through the eyes and the longitudinal direction of the carapace of the *euphausiids*. The frequency distributions of tilt angles have been derived from photographs of free-swimming krill at different hours.

2. The results and discussion

Figure 5 shows the results from two of our observations at a time interval of about 5 min. The frequency distribution of the tilt angles yields a mean value for the tilt angle of −9.8° with a standard deviation of 34.1°. This means that the major part of the krill is tilted downwards at this depth, 40 m and time, 0200 h. Simultaneous observations with a 120-kHz echo-integrating system showed a downward migration of the plankton layer at that depth and hour.

In most of our pictures the standard deviation of the tilt angle distribution is estimated to be between 25°–45°. The mean value changes from slightly positive to slightly negative during the day. The sign of the mean value seems to be highly correlated to the migration process of the krill community. The data which will be used in the abundance estimation of krill were all collected when the krill swarms were at their most shallow depth, at midnight, where no vertical migration took place. Thus in our model we will use a Gaussian tilt-angle frequency distribution, with zero mean and a standard deviation of 30°, when estimating zooplankton size distribution and abundance.

III. ESTIMATION OF SIZE DISTRIBUTION AND ABUNDANCE OF ZOOPLANKTON

A. An empirical scattering model

Two other investigations, on measurements of target strength of marine zooplankton at several frequencies, have been reported. One of these works[7] is on the krill species *Euphausiia pacifica*. The backscattering spectra of Greenlaw's measurements are very similar to our measurements, at low and medium frequencies.

The other work[11] is on mixtures of different kinds of free-swimming zooplankton at sea. The dominant species were *calanoid copepods*, from which Holliday and Pieper[11] measured the volume-backscattering strength at four fre-

TABLE I. Sound speed contrasts for different species of zooplankton.

Species	Number of measurements n	Mean sound speed contrast h	Sample standard deviation
M. norvegica	3	1.035	0.0061
Thysanoessa	5	1.025	0.0047

quencies, 0.54, 1.16, 1.80, and 3.08 MHz. In all measuring series they observed an increasing scattering strength, as a function of frequency, at the three lowest frequencies. Furthermore, the scattering strength at 3.08 MHz, for all measuring series, was lower than the scattering strength at 1.8 MHz. In most of the measuring series it was also lower than the observed scattering strength at 1.16 MHz. It is impossible to estimate a size distribution which will generate the observed dependence of the volume-backscattering strength on frequency, from a model which predicts a monotonic increase in the target strength, as the Johnson model does.

The predicted target strength from the Johnson model is equal to the maxima predicted by the Anderson model, in the high-frequency region. The measured target strengths, for both size classes, were approximately 6 dB higher than those predicted by the Johnson model. Hence, the Anderson model will also predict target strengths that are too low. The increase in the measured target strengths, compared to the predicted values, is in a proper direction to account for the impact of adding a carapace or exoskeleton to the fluid sphere approximation. In order to achieve satisfactory accordance between predictions based on the Johnson model and measured volume-backscattering strength, Holliday and Pieper[11] had to apply very high values for the contrasts, g and h. Thus their observation is in the same direction as ours, i.e., the measured volume-backscattering strength is higher than predicted by the Johnson model. Furthermore, neither of the fluid sphere models can predict an orientation dependence of the target strength. Due to these facts we conclude that a fluid sphere is insufficient as a scattering model for *euphausiids*.

The functional form of the measured backscattering cross section of krill has some of the same characteristics as a second-order high-pass filter, with complex conjugated poles. We will therefore use an expression similar to that of a second-order high-pass filter as an empirical scattering model for krill and tune the amplitude and the location of the resonance frequency to our experimental results. This empirical model for the backscattering cross section versus frequency can be written as

$$\sigma_{bs}(f) = C \frac{a^2}{[(f_0/f)^2 - 1]^2 + \partial^2} d(f,a,\varphi), \qquad (5)$$

where

C,∂ = model parameters,
f_0 = the resonance frequency,
a = equivalent radius,
d = backscattering cross-section orientation function,
φ = tilt angle.

The coefficient C will determine the scattering strength in the high-frequency domain, while the damping constant ∂ determines the Q value of the resonance at the frequency f_0.

In our empirical model we want to reflect the functional dependencies of varying density and sound speed contrasts. This can be done by including the constant term of the first-order approximation of the Anderson model, i.e., in the Rayleigh scattering zone, in the parameter C of Eq. (5). This term is also included in the Johnson model. In the geometric scattering domain the measured backscattering cross sec-

tions were approximately four times (6 dB) higher than those predicted by the Johnson model. Thus we have to apply a multiplication factor in order to fit the experimental data to our model. This multiplication factor might be considered as a correction factor to account for the influence of the carapace and is put equal to four. The expression for C of Eq. (5) can now be written as a function of the density contrast g and the sound speed contrast h, i.e.,

$$C = 4 \left(\frac{1 - gh^2}{3gh^2} + \frac{1 - g}{1 + 2g} \right)^2. \qquad (6)$$

The equivalent radius is given by Eq. (3). From our data we find that a proper value of ∂ is between 0.5 and 0.7. In this work we will use $\partial = 0.5$.

The last factor to be determined in Eq. (5) is the resonance frequency f_0. We concluded previously that the measured resonance frequency was shifted downward, in frequency, to about 50% of the predicted transition region from the fluid sphere model. Thus we will let the resonance frequency be determined by $ka = 0.5$, which gives $f_0 = c/4\pi a$.

In order to make reliable estimates of the zooplankton abundance it is necessary to include the directional characteristics of the scattering from krill in our empirical model. This may be done by regarding the backscattering from a krill as the acoustic radiation from a line source. The beamwidth of a line source is given by

$$\theta_0 \approx 0.9(\lambda/L), \qquad (7)$$

where

λ = the wavelength of the sound

and

L = the length of the line source.

The theoretical beamwidth, Eq. (7), of a line source of length 43 mm and the measured main-lobe width of a 43-mm krill, from Fig. 4, is given in Table II.

It is most important to correct for the directive scattering from krill at the highest frequencies. At these frequencies the beamwidth of the line source and the measured main-lobe width of the krill are of approximately the same size.

Thus we will use a backscattering cross-section orientation function $d(f,a,\varphi)$ for the backscattering from krill, similar to the directivity function of a line source, which can be written as

$$d(f,TL,\varphi) = \left(\frac{\sin[\pi(TL/\lambda)\sin\varphi]}{\pi(TL/\lambda)\sin\varphi} \right)^2. \qquad (8)$$

TABLE II. The theoretical beamwidth of a line source of 43-mm length and the measured width of the main lobe of a 43-mm krill at three frequencies.

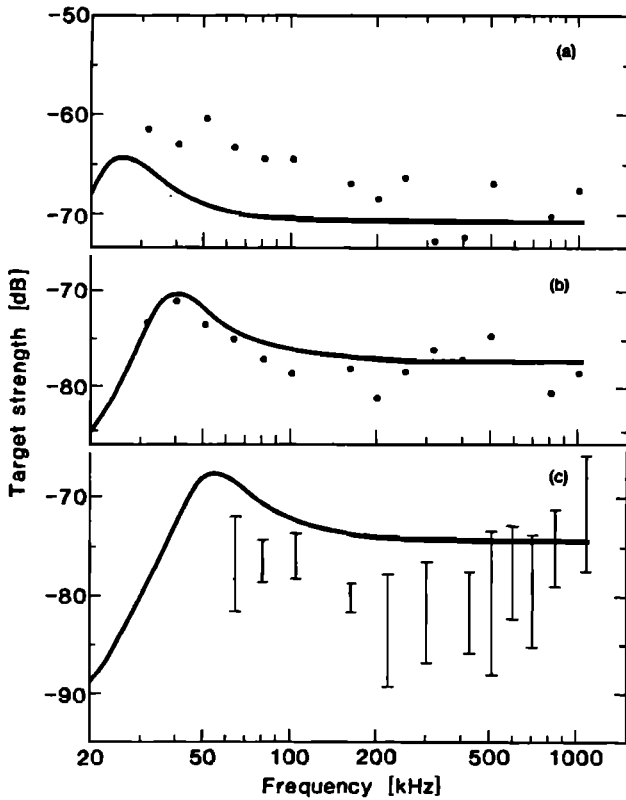| Frequency (kHz)	Beamwidth of a line source L = 43 mm (deg)	Width of the main lobe of a krill; TL = 43 mm (deg)
40	43.7	30
80	21.7	18
315	5.6	7

FIG. 6. The target strength of krill versus frequency. The dots are the mean values of the measured data and the solid lines are the predictions from our empirical model. (a) 40-mm mean bodylength, $g = 1.034$, $h = 1.035$. (b) 27-mm mean bodylength, $g = 1.023$, $h = 1.025$. (c) Experimental results of Greenlaw, 23-mm mean bodylength, $g = 1.063$, $h = 1.033$.

Our complete empirical model will thus be given by Eqs. (5)-(8).

Our experimental data along with the predicted target strength from our empirical model are shown in Fig. 6. The experimental results of Greenlaw's[7] investigation are also shown in Fig. 6. In his paper, Greenlaw mentioned that the peak values are probably the best estimates of the target strength.

From Fig. 6 we find that our empirical model fits the available experimental data on krill quite well, both for the 27-mm bodylength krill of our work, and for the 20-mm bodylength krill of Greenlaw's work. The accordance between the model's measurements and ours, on the 40-mm bodylength krill, is poorer, but the target strength, in the high-frequency region, is much better predicted by our model than by any of the fluid sphere models.

In Figs. 7 and 8 the mean target strength versus frequency of a krill of 40-mm length, as computed from Eq. (1), is given. In Fig. 7 the spatial orientation was modeled by a Gaussian tilt-angle distribution with a mean value of 0° and various standard deviations. In Fig. 8 the mean tilt-angle value is varied from 0°–40°, with a constant standard deviation of 30°.

In the literature, diurnal variation of the mean volume-backscattering strength has been reported by Everson.[24] He measured a change in the volume-backscattering strength, at 120 kHz, of up to 8.5 dB between day and night, with the highest strengths occurring during the daytime. The observed krill size was approximately 44 mm. Everson observed that, during the daytime, the krill were aggregated into compact swarms, while during the night they were dispersed in the water. Thus it is probable that the orientation distribution changed from night to day and that the standard deviation is larger in dispersed-plankton swarms than it is in more aggregated swarms. If we assume a Gaussian orientation distribution, with zero mean at both day and night, we find, from Fig. 7, that a change in the standard deviation from 10°–40° results in a reduction of the mean target strength of about 5 dB at 120 kHz for krill of 44-mm bodylength. This indicates that if we take into account the orientation-dependent target strength, the observed change in the
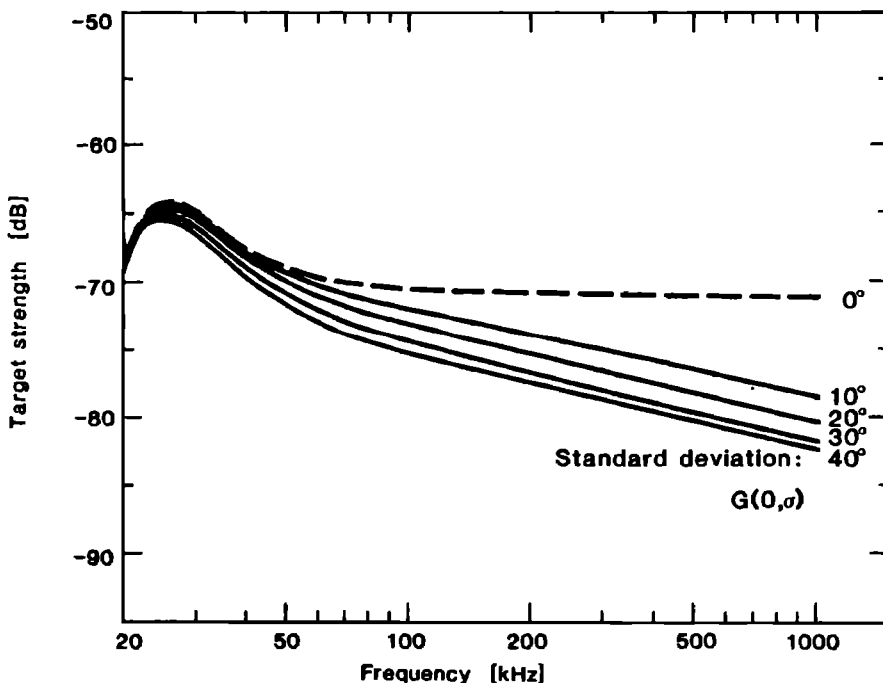

FIG. 7. The mean target strength versus frequency of a 40-mm bodylength krill calculated from Eq. (5). The Gaussian orientation distribution function has zero mean and the standard deviation is given as a parameter.
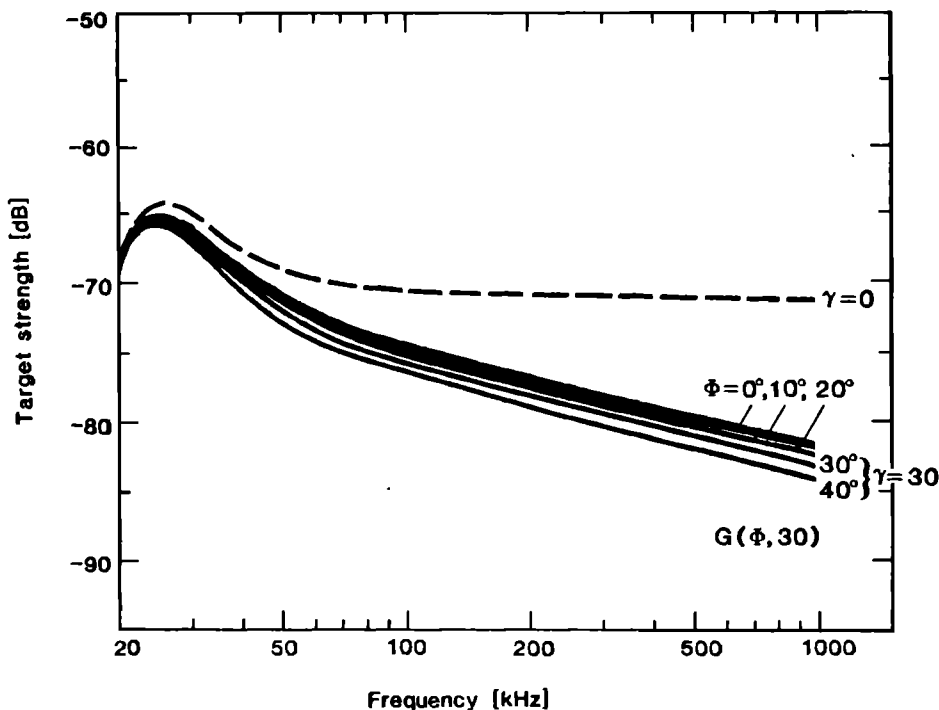
FIG. 8. The mean target strength versus frequency of a 40-mm bodylength krill calculated from Eq. (5). The Gaussian orientation distribution function has a standard deviation of 30°, and the mean value is given as a parameter.

volume-backscattering strength from daytime to nighttime can be explained by a changed standard deviation of the orientation distribution from an aggregated to a dispersed plankton swarm.

B. Estimation of size distribution of zooplankton

1. The acoustic and biologic data acquisition method

The measurements of the volume-backscattering strength were performed from the RV "JOHAN RUUD," in the Tromsø area, in August 1982. The data were collected using a modified version of the equipment that was applied in the backscattering cross-section measurements of individual krill, presented previously. In these measurements the transducers were mounted in a plane frame. The frame could be faced either sideward or downward.

It is known that sequential measurements of the backscattered intensity, from a water volume containing moving scatterers, yield a sequence of fluctuating measured values. Thus the measured volume-backscattering coefficients, which we want to apply in the acoustical size-distribution estimation, are stochastic quantities.[25] Therefore, we have to use measured mean values of the volume-backscattering coefficients of Eq. (5). This implies that our measured data will be subject to random errors, due to a mean value based on a finite number of measurements. To meet the requirements of acceptable variance,[18] we averaged the square of the received signal and corrected for spherical spreading over a 15-m-depth interval in the plankton layer from each pulse transmission. The mean volume-backscattering strength, in the estimation procedure, is averaged over 25 transmissions.

On the occasion when we achieved the best signal-to-noise ratio, the plankton layer was at a depth of 50–70 m. The transducers were lowered to a 45-m depth, facing down-

ward. This measuring series resulted in a signal-to-noise ratio, between 5–20 dB, at the different frequencies, and at a distance of 5–20 m from the transducers.

There was no simultaneous acoustic and biologic sampling of the plankton layer. However, several biological samples were collected in the nearby Ullsfjorden the same day. The biological sampling was done by a 1-m^2 opening Tucker trawl,[26] with a plankton net of 1-mm mesh size, a pelagic trawl having an opening of 18 × 18 m, and fine-meshed net in the cod end.

2. The estimation method

From Eq. (6) the number of organisms per m^3, N, can be estimated from measurements of the volume-backscattering coefficient, s_v, if the mean backscattering cross section, $\bar{\sigma}_{bs,m}(f)$, and the length-frequency distribution, l_m, are known. In principle, the length-frequency distribution l_m can be derived acoustically if the volume backscattering strength is measured as a function of frequency.[27] In a multi-frequency formulation, Eq. (2) can be written as

$$S = \sum_{bs} \times N, \tag{9}$$

where

S = the measuring vector with the elements $s_v(f_i)$, for the volume-backscattering strength at frequency i,

$\sum_{bs}$ = the $I \times M$ scattering matrix with the elements $\bar{\sigma}_{bs,m}(f_i)$, as the backscattering coefficients. The variables I and M are the number of measuring frequencies and size classes, respectively,

N = the number vector with elements n_m, as the number of scatterers of size group m.

An estimate of the zooplankton size distribution for the wa-

ter volume considered is obtained if Eq. (9) can be solved. The existence of any solution at all is determined by the coefficients of the matrix Σ_{bs}.

A solution method of such problems is the least-square minimizing procedure.[28] In size estimation of zooplankton we can add the restriction to the solution that none of the size groups contains a negative number of scatterers and apply an algorithm for solving non-negative, least-square, NNLS problems.[29] This method of extracting biophysical information from the acoustic signature of the backscattered intensity has been used by several authors.[8,30–32]

The choice of the NNLS algorithm, as our inversion method, was motivated by the relatively low signal-to-noise ratio we achieved with the acoustic system, the inherent instability in the inversion problem, and its usefulness for both under- and over-determined problems, i.e., for both $I > M$ and $I < M$ in Eq. (9).

3. Results and discussion

The results are given mainly to indicate the influence of the different scattering models on the estimated size distribution, rather than to give a comprehensive validation of the method or one of the models.

The species composition were similar in all net samples analyzed. Hence, we assume that the plankton layer, on which we carried out the acoustical measurements, consisted of the same species as those found in the trawls. (The results of the biological samples are given in Fig. 9.)

It is seen from Fig. 9 that the krill community consisted of three size classes with a mean bodylength of 9, 17, and 32 mm. The two smallest size classes were a mixture of the two *Thysanoessa* species, while the largest size class was *M. norvegica*. A minor number of other, smaller, zooplankton species, mainly *calanoid copepods*, were also present in the net samples, but there were too few of these specimens to be illustrated in Fig. 9.

Inversion was accomplished using each of the three scattering models, the Johnson model, the Anderson model, and our empirical model. The results are presented in Fig. 10.

When applying the Johnson model, in the inversion procedure, the acoustically estimated size distribution contains only one size class, with a bodylength of about 43 mm, as can
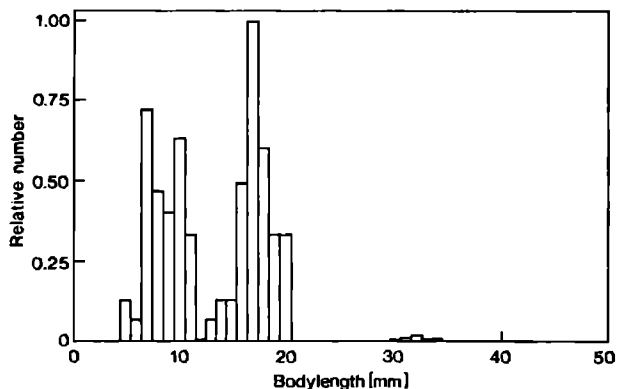

FIG. 9. The relative length frequency distribution of krill from the trawl samples from Ullsfjorden.
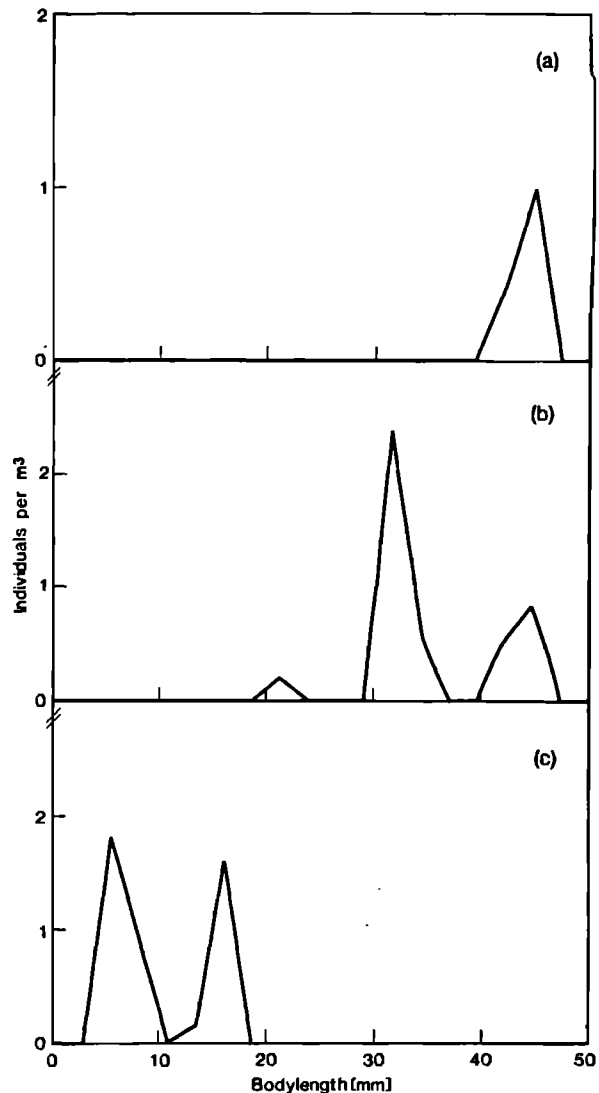
FIG. 10. Acoustically estimated length frequency distribution based on three scattering models. (a) The Johnson model, (b) the Anderson model, (c) our empirical model.

be seen in Fig. 10(a). This is because the Johnson model does not reflect a decreasing volume-backscattering strength versus frequency. In this case, the best fitted size distribution to the measured values, therefore, contains only one size class, which approximately corresponds to the global maximum of the volume-backscattering strength function. A bodylength of 43 mm corresponds to a transition region, $ka = 1$, at about 50 kHz, while the observed global maximum is at 63 kHz.

By applying the Anderson model, we obtain the acoustically estimated size distribution of Fig. 10(b). This distribution contains three different size groups of about 21, 31, and 44 mm. There is a better accordance between this size distribution than the one estimated by the Johnson model, compared to the results of the biological samples. However, the acoustically estimated size distribution results in size classes with larger bodylengths than those from the trawl samples. This is expected, since our measurements of the target strength of a single krill indicate that the transition region from Rayleigh to geometric scattering is shifted to about half of the frequency predicted by the fluid sphere models. Using

TABLE III. The estimated biomass per m³ of the different size groups of Fig. 10(c).

Krill bodylength (mm)	Mean number of individuals per m³ 50–65-m depth	Mean biomass per m³ 50–65-m (mg)
5.3	1.8	2.1
7.9	0.8	2.2
13.2	0.2	2.7
15.8	1.6	36.8

scattering models, which do not take into account this observation, the result will be a size distribution containing size classes with too large a bodylength.

If we apply our empirical model, we obtain the results illustrated in Fig. 10(c). This distribution contains two size groups with about a 6- and a 16-mm bodylength. There is good accordance between this size distribution and the results from the trawl samples. The most distinct discrepancy is the lack of a size group with a 32-mm mean bodylength. However, this size group contains very few specimens and will, therefore, only be responsible for a small contribution to the total volume-backscattering strength. In addition, the estimated resonance frequency, for a krill with a 32-mm bodylength from our empirical model, will be at 32.5 kHz, which is at the very low end of the frequency range of our measuring equipment. Thus our measuring equipment is not sufficient for the measurement of zooplankton with a bodylength larger than 30 mm.

Based on the acoustically derived size distribution, our empirical model, the volume-length relation, and the measured specific density, we may compute the biomass per m³. The result is given in Table III. The total biomass per m³, estimated by the acoustical method, at the particular location of Ullsfjorden was 43.8 mg.

We have not performed any biomass estimate based on the data from the net samples. This has not been done since the catch efficiency of the different zooplankton trawls is unknown and strongly variable for different trawls.[33] We assume, however, that the size distribution can be derived from the net samples, since different trawls gave approximately the same size distribution, but very different biomass estimates.

IV. CONCLUSION

The target strength versus frequency was measured for two species and two size classes of krill and versus aspect angle of the organism. From this it was concluded that the fluid sphere was insufficient as a scattering model for krill. This was based on the observed resonance-like behavior of the target strength at $ka \approx 0.5$ and that krill are highly directive scatterers.

The measurements of the specific density of krill showed that the density contrast was a function of the bodylength of the organisms. The measurements of the sound speed yielded different values of the sound speed contrast for the species concerned.

Observation of the tilt-angle distribution, of free-swim-

ming krill at sea, showed that krill were distributed over a large region of tilt angles. Since krill are directive scatterers, this fact must be taken into account when reliable abundance estimates are done using acoustical methods.

Our empirical model predicts a decreasing target strength versus frequency in the geometric scattering region which is consistent with reported results in the literature on other species of marine free-swimming zooplankton. The parameters of the model were determined by a best fit procedure. The observed directivity of krill was also included in the model. We conclude that the backscattering spectra of zooplankton are better described by our empirical model than by the fluid sphere models. Adjustments of the parameters of the model may be necessary when other zooplankton species are concerned.

Using the empirical model, the dominant size groups from the trawl catches were present in the acoustically estimated size distribution.

[1]J. H. Steele, "Patchiness," in *The Ecology of the Seas*, edited by D. H. Cushing and J. J. Walsh (Blackwell, Oxford, England, 1976).

[2]R. M. Cassie, "Sample design," in *Zooplankton Sampling*, edited by D. J. Tranter and J. H. Fraser (UNESCO, Paris, France, 1968).

[3]M. Vannucei, "Loss of organisms through the meshes," in *Zooplankton Sampling*, edited by D. J. Tranter and J. H. Fraser (UNESCO, Paris, France, 1969).

[4]R. E. Pieper, "Euphausiid distribution and biomass determined acoustically at 102 kHz," Deep Sea. Res. 26, 687–702 (1979).

[5]V. C. Anderson, "Sound scattering from a fluid sphere," J. Acoust. Soc. Am. 22, 426–431 (1950).

[6]R. K. Johnson, "Sound scattering from a fluid sphere revisited," J. Acoust. Soc. Am. 61, 375–377 (1977).

[7]C. F. Greenlaw, "Backscattering spectra of preserved zooplankton," J. Acoust. Soc. Am. 62, 44–51 (1977).

[8]C. F. Greenlaw, "Acoustical estimation of zooplankton populations," Limnol. Oceanogr. 24, 226–242 (1979).

[9]C. S. Clay and H. Medwin, *Acoustical Oceanography* (Wiley, New York, 1977), p.181.

[10]Å. Kristensen and J. Dalen, "Measurements of acoustical backscattering strength from euphausiids (krill)," in *Ultrasonics International 81 Conference Proceedings*, Brighton, U. K. (IPC Sci. Tech. Press, London, 1981), pp. 160–164.

[11]D. V. Holliday and R. E. Pieper, "Volume scattering strengths and zooplankton distributions at acoustic frequencies between 0.5 and 3 MHz," J. Acoust. Soc. Am. 67, 135–146 (1980).

[12]Lord Rayleigh, *The Theory of Sound* (Dover, New York, 1945), Vol. II, pp. 272–284A.

[13]C. Yeh, "Scattering of acoustic waves by a penetrable prolate spheroid. I. Liquid prolate spheroid," J. Acoust. Soc. Am. 42, 518–521 (1967).

[14]W. M. Visscher, "A new way to calculate scattering of acoustic and elastic waves II," J. Appl. Phys. 51, 835–845 (1980).

[15]C. L. Bennett and H. Mieras, "Time domain integral equation solution for acoustic scattering from fluid targets," J. Acoust. Soc. Am. 69, 1261–1265 (1981).

[16]U. Kiils, "Preliminary data on volume, density, and cross section area of Antarctic krill, *Euphausia superba,*" Meeresforsch. 27, 207–209 (1979).

[17]N. Payne and C. E. Stephenson, "Measuring the density of polyolefins. An improved gradient column," Mat. Res. Stand. 4, 3–7 (1964).

[18]Å. Kristensen, "Acoustic classification of zooplankton," Ph.D. thesis (Norwegian Institute of Technology, Trondheim, Norway, 1983).

[19]S. Falk-Petersen, "Ecological investigations on the zooplankton community of Balsfjorden, northern Norway: Seasonal changes in the bodyweight and the main biochemical composition of *Thysanoessa inermis* (Krøyer), *T. raschii* (M. Sars), and *Meganyctiphanes norvegica* (M. Sars) in relation to environmental parameters," J. Exp. Mar. Biol. Ecol. 49, 103–120 (1981).

[20]S. Falk-Petersen, R. R. Gatton, J. R. Sargent, and C. C. E. Hopkins, "Ecological investigations on the zooplankton community in Balsfjorden, northern Norway: Seasonal changes in the lipid class composition of *Meganyctiphanes norvegica* (M. Sars), *Thysanoessa raschii* (M. Sars), and *T. inermis* (Krøyer)," J. Exp. Mar. Biol. Ecol. 54, 209–224 (1981).

[21]P. C. Beamish, "Quantitative measurements of acoustic scattering from zooplankton organisms," Deep Sea Res. 18, 811–822 (1971).

[22]U. Kiils, "Schwimmverhalten, Schwimmleistung, und Energiebalanz des Antarktischen Krills *Euphausia Superba,*" Ber. Inst. Meeresk. Kiel 65, 1–72 (1979).

[23]D. D. Sameoto, "Quantitative measurements of euphausiids using a 120 kHz sounder and their *in situ* orientation," Can. J. Fish. Aquat. Sci. 37, 693–702 (1980).

[24]I. Everson, "Diurnal variation in the mean volume backscattering strength of an Antarctic krill (*Euphausia superba*) patch," J. Plank. Res. 4, 155–162 (1982).

[25]B. F. Cron and W. R. Schumacher, "Theoretical and experimental study of underwater sound reverberation," J. Acoust. Soc. Am. 33, 881–888 (1961).

[26]D. D. Sameoto and L. D. Jarosynski, "Some plankton net modifications and developments," Fish Mar. Ser. Res. Dev. Tech. Rep. 697, p. 35 (1976).

[27]C. F. Greenlaw and R. K. Johnson, "Multiple-frequency acoustical estimation," Biol. Oceanogr. 2, 227–252 (1983).

[28]J. N. Franklin, *Matrix Theory* (Prentice–Hall, Englewood Cliffs, NJ, 1968), pp. 50–55.

[29]C. L. Lawson and R. J. Hanson, *Solving Least Square Problems* (Prentice–Hall, Englewood Cliffs, NJ, 1974), pp. 160–165.

[30]D. V. Holliday, "Extracting bio-physical information from the acoustic signatures of marine organisms," in *Oceanic Sound Scattering Predictions,* edited by N. R. Anderson and B. J. Zahurance (Plenum, New York, 1977), pp. 619–624.

[31]A. Løvik and J. M. Hovem, "A new echosounder for measurements of length distribution of shoaled fish," in *Electronics for Ocean Technology,* IERE Conference Proceedings No. 51, Birmingham, U. K. (IERE, London, 1981), pp. 321–327.

[32]A. Løvik and Å. Kristensen, "Acoustic classification of marine organisms," Int. Coun. Explor. Sea CM, B:18, 9 pp. (Mimeo) (1981).

[33]S. Falk-Petersen and Å. Kristensen, "Acoustic assessment of krill stocks in Ullsfjorden, North Norway," Sarsia 70, 83–90 (1985).